ISSN No:-2456-2165

An Intelligent System to Analyze the Functional Magnetic Resonance Imaging fMRI

George Karraz [12]
[1] Department of Artificial Intelligence & Natural Language Processing, Faculty of Information Technology Engineering, Damascus University.
[2] Department of Informatics, Faculty of Engineering, Al-Sham Private University, Damascus, Syria.

Abstract:- A Lot of medical projects aim to combine biology with computer science like artificial limb which is able to simulate real limb's activities to some extent, and that requires to comprehend the neurological map of the brain. The best way to measure the brain's activity is Functional Magnetic Resonance Imaging (fMRI), where it is a functional neuroimaging procedure using MRI technology that measures brain activity by detecting changes associated with blood flow. In this paper we develop an automatic system based on soft computing methods, to analyze fMRI Images and conclude their proper intended behavior. Our data was composed from two parts, the major part was obtained from the famous dataset (A test-retest fMRI dataset for motor, language and spatial attention functions), which has a representation of five different behaviors "finger foot and lip movement, overt verb generation, covert verb generation, overt word repetition and landmark tasks", where the second part was prepared by us using images that free downloaded from internet network. Our developed automatic classification system is based on neural network framework, which is proceeding in two stages:

1. The first stage extracts four specific features, through applying sophisticated techniques for automatic image processing and analysis, related to the presence of different intensity values and their addresses over the 2 dimensions studied images. The selected features were unique and contribute to make our system, good represented.

2. The second stage is a classification technique, through designing a suitable artificial intelligence system architecture and learning algorithm. We did a lot of experiments in order to select the best neural network architecture and training method, the experiments proved that the best performance was achieved in three layers neural network: input, hidden and output layers, with a training method based on Back propagation algorithm, and sigmoid activation function. Developed system achieved an accuracy of 94.4%.

Keywords:- *fMRI; Neural Networks; Brain Activity Automatic Interpretation; Fuzzy C-maen clustering; Linear Regression.*

I. INTRODUCTION

Japanese S.Ogawa [16] was the first to discover the technique of functional magnetic resonance imaging (*f*MRI) in 1990. Ogawa discovered that the magnetic properties of blood vary with the percentage of oxygen in it. At the end of his research, Ogawa predicted that this method could be used to measure brain activity by taking advantage of the difference in the amount of oxygen in the blood when cells perform a certain activity compared to other cells. Ogawa has done more research to prove that his method can be successful in measuring brain activity, shared by many scientists in the world. Indeed, the effectiveness of this method has been proven and developed to become the most important tool in revealing the secrets of the brain.

In the last ten years, the use of this technology has increased significantly, especially in the field of studying the brain and its functions and related research. Studying the functions of the brain and how it functions is a difficult challenge, because the brain is fortified within strong bones for its protection (the bones of the skull). Scientists have developed many ways to study the brain, but *f*MRI technology may be the most important of these methods because it is safe and does not include any radiation or any interference surgical. In addition to the research applications of *f*MRI, its use in the clinical field in hospitals and its applications in them is increasing, especially in pre-surgery cases of the brain.

We know a lot about the brain before the advent of *f*MRI using different methods of studying the brain, perhaps the oldest is postmortem autopsy. For example, Broca's area of the brain (responsible for speech and pronunciation) was discovered by autopsying the brain of a person who was healthy, but then contracted a disease (what is known today as a stroke) and lost the ability to speak. The brain of this person was dissected after his death by the doctor Paul Broca [1] and it was discovered that there was a death of cells in the brain in a certain area, the doctor concluded that this area is responsible for speech, after that indeed subsequent experiments proved the correctness of his words and this area was named after Broca's area. The brain is made up of several regions that have different and varied functions. Research on brain functions is still trying to understand the brain, and although we know a lot about the brain and its secrets, there is also a lot that we don't know. Let's take another famous example,Wernicke's area [2], which is a region of the brain responsible for understanding speech. For example, any disease in Wernicke's area may result in the patient speaking in an incomprehensible

language. He may speak well because Broca's area is not affected, but his words have no meaning.

The brain is interconnected with each other and there is no region that can perform its functions on its own, so a specific region of the brain may have multiple functions, or the function may be performed by several regions of the brain. We must therefore be careful when interpreting the *f*MRI results. For example, Broca's area alone cannot produce speech, but we need other areas of the brain responsible for the movement and coordination of muscles in the face, wemay also need the area responsible for memory toretrieve memorized words from it. Figure 1 illustrates the functional division of the surface cerebral cortex as it reported by H. Whitaker [10].

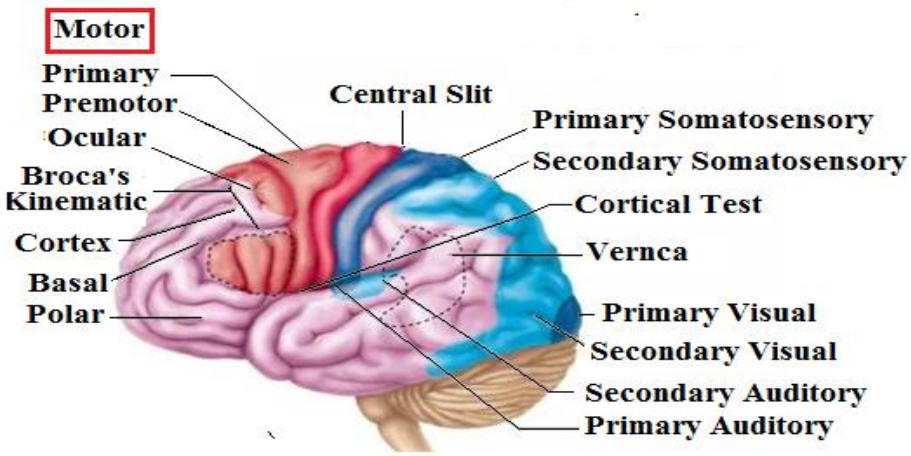

Fig. 1: The functional division of the surface cerebral cortex

II. RELATED WOEKS

C. Candemir [5] presented a two-fold innovative study. First, detection algorithms to locate the activations in *f*MRI signals. Furthermore, proposed and compared a set of change points (CP) analysis methods, such as a regression-based method (RBM), a statistical method (SM), and a method that based on the mean difference of double sliding windows (MDSW)) to locate such points (CP).

Secondly, these methods were applied on the *f*MRI signals, which are acquired from the real subjects, while they were performing *f*MRI tasks. Proposed methods were applied to three different *f*MRI experiments with a motor, a visual and a linguistic tasks. The analysis shows that the methods find activations in accordance with established techniques such as statistical parametric maps (SPM). The acquired results showed accuracy up to 94 %, also showed that the proposed techniques can be used effectively to locate the activation times on *f*MRI time series.

M. H. Lee [15], investigated the differential spatial covariance pattern of blood oxygen level-dependent (BOLD) responses to single-task and multitask functional magnetic resonance imaging (*f*MRI) between patients with psychophysiological insomnia (PI) and healthy controls (HCs), and evaluated features generated by principal component analysis (PCA) for discrimination of PI from HC, compared to features generated from BOLD responses to single-task *f*MRI using machine learning methods. In 19 patients with PI and 21 HCs, the mean beta value for each region of interest (ROIbval) was calculated with three contrast images (i.e., sleep-related picture, sleep-related sound, and stroop stimuli). They performed discrimination analysis and compared with features generated from BOLD responses to single-task *f*MRI. They applied support vector machine analysis with a least absolute shrinkage and selection operator to evaluate five performance metrics: accuracy, recall, and specificity. Principal component features showed the best classification performance in all aspects of metrics compared to BOLD response to single-task *f*MRI. The approach showed better performance in discriminating patients with PI from HCs, compared to single-task *f*MRI.

H. Hasan [9], analyzed the underlying causes of the limited performance of the projected density algorithm when applied to brain data. In addition, compared it with an approach that relies on the optimization of the conductivities of a small number of tissue compartments of anatomically detailed head models, which reconstructed from structural MR data. Both for simulated ground truth data and magnetic resonance current density imaging MRCDI data, the obtained results indicated that the estimation of densities benefits more than using a personalized volume conductor model. In particular, they introduced a hierarchical statistical testing approach as a principled way to test and compare the quality of reconstructed current density images that accounts for the limited signal-to-noise ratio of the human in-vivo MRCDI data and that the ground truth of the current density is unknown for measured data. The results indicated that the statistical testing approach constitutes a valuable framework for the further development of accurate volume conductor models of the head. The findings also highlight the importance of tailoring the reconstruction approaches to the quality and specific properties of the available data.

K. J. Gorgolewski [12], found that the adaptive threshold can improve reliability, mainly by accounting for the general signal variance. This in turn increases the likelihood that the true activation pattern can be determined

offering an automatic yet flexible way to threshold single subject *f*MRI maps.

B.A. Kirchhoff [4] had adopted a study that reveals functional anatomic correlates of verbal and perceptual strategies that are variably used by individuals during encoding. These strategies engage distinct brain regions and may separately influence memory performance.

K. J. Duncan [11] proposed a technique based on a statistical methodology, aiming to evaluate the consistency, associated with functionally localizing reading- and object-sensitive in areas of left occipital-temporal cortex. The obtained results were closely match previous studies with peak activations located in the posterior occipital-temporal sulcus according to the written words. Then concluded that intra-subject variability was surprisingly high, with between one third and three quarters of the voxels in a given image not corresponding to those activated in the main task. This level of variability stands in striking contrast to the consistency seen in retinotopically defined areas and has important implications for designing robust but efficient functional localizer scans.

G. Ganis [8] found that *f*MRI revealed that well-rehearsed lies that fit into a coherent story elicit more activation in right anterior frontal cortices than spontaneous lies that do not fit into a story, whereas the opposite pattern occurs in the anterior cingulate and in posterior visual cortex.

D. K.Jones [7] had shown through their study that it is possible to obtain robust and high quality diffusion tensor MR data at 1.5 Tesla with isotropic resolution (2.5 × 2.5 × 2.5 mm) from the whole brain within a sufficiently short imaging time that it may be incorporated into clinical imaging protocols.

III. PROBLEM DICRIPTION

There have been many serious attempts to analyze (*f*MRI) images, to isolate the active zones presented in the image, in order to proceed an automatic interpretation of what is associated with these zones of behaviors according to their locations within the map of the brain image. The problem of our research is to use more of effective techniques in the fields of analysis and automatic interpretation of the studied image, based on the artificial intelligence algorithms, to achieve, as possible as, better results in accuracy of our developed system, in comparison to our peer researches.

IV. MOTIVATION AND OBJECTIVE

The main motivation behind this research is to present a new initiative in the subject of automated analysis of *f*MRI images, in the first stage of research, using two parallel mechanisms of artificial intelligence algorithms, where the developed mechanisms showed equal high efficiency in separating activation zones in the studied images. In addition, the two developed mechanisms have greatly contributed to support the second stage of our research, which is the automatic interpretation of behaviors related to the activated zones in the image, we ensure that the main reason for increasing accuracy of image interpretation isrelated mainly, to the two developed techniques of image automatic analysis.

V. PROPOSED WORK

A. fMRI Images Processing

The *f*MRI image was represented in 2D and in grayscale mode using the functions designated for this purpose in Matlablanguage, then we developed two different adaptive approaches to analyze automatically the studied *f*MRI images in our dataset, in order to isolate the activated zones from other details presented in the images.

The 1st approach is an intelligent model based on linear regression that operates to determine an adaptive appropriate threshold according to the gray intensity, in an attempt to facilitate the isolation of active zones using this type of medical imaging. Through our observations to the images presented in the studied dataset, we concluded that it's very important to use the statistics features that could be calculated over all of image intensity values (maximum, mean and standard deviation), this technique gave us the possibility to calculate an important statistical factor (X) that affects in estimating the threshold in the developed approach, so the linear regression model takes X as input, where the output is the threshold value.

The 2nd approach based on the using of Fuzzy C-means Clustering algorithm (fcm), in order to determine the centroids for every cluster of intensity values in *f*MRI image, It's clearly noted that every activated zone correspond to a specific centroid and cluster, here we used the Z-Scores as a statistical representation, to specify the number of *f*MRI image clusters which are needed in fcm operation. In our two developed approaches we extract coordinates of detected activated zones in *f*MRI images, in order to achieve our target, in classifying the presented behaviors in the brain regions.

- *Linear Regression Model:*

The linear regression model [6] is our first approach to reveal the correct adaptive threshold to isolate the activation zones in *f*MRI image, firstly we divided our dataset in two parts, the first part forms 60% of total images and the second one forms 40%, the first part forms training dataset, and the second part forms the testing dataset, the process began to represent all 2D images in our database graphically in 3D, in order to illustrate the intensity values of studied image on Z-axis, and the coordinates of image on X-axis and Y-axis, Figure 2 illustrates the *f*MRI image and the manner of its representation.

Then we created a target vector corresponds to threshold values of the activated zones in images, for every image we specified an adaptive threshold, the created vector (Y) represents the regression model target in the training stage, the input of model (X) is a vector of features, that can be calculated from three specified statistical values extracted from all studied *f*MRI images, (maximum (MAX), average (MEAN) and standard deviation (STD)), as illustrated in Equation 1

ISSN No:-2456-2165

$$X = \frac{MAX_{Val} - Mean_{val}}{STD_{Val}} (1)$$

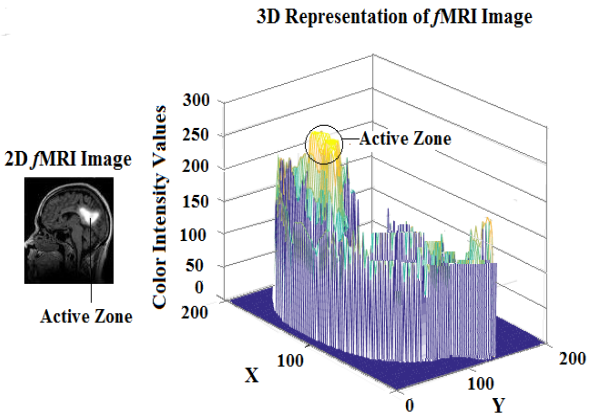

Fig. 2: *f*MRI image and its 3D representation

Our linear regression model (LR) depend on three main elements, the first element is the hypothesis of linear function which is illustrated in Equation 2.

$$h(x) = \theta_0 + \theta_1 x \quad (2)$$

Where h(x), x,θ_0 and $\theta_1$represent the estimated output, input, weights of linear model, respectively.

The second element in linear regression model is the cost function which is used in optimization process, in this model we used the mean squared error (MSE) as a cost function as reported in Equation 3.

$$J(\theta_0, \theta_1) = \frac{1}{2m} \sum_{i=1}^{m} (h_\theta(x^{(i)} - y^i)^2 \quad (3)$$

The third element in linear regression model is the optimization method, we use the Gradient Descent (GD) algorithm in order to minimize the cost function and find the best hypotheses that reveals the accurate solution of our problem to determine the adaptive threshold in order to isolate the activation zones in *f*MRI image. The (GD) function is illustrated in Equation 4.

$$\theta_j = \theta_j - \alpha \frac{\partial}{\partial \theta_j} J(\theta_0, \theta_1)$$

$$\text{for } j = 0 \text{ and } 1 \quad (4)$$

Where: α is the learning rate which may be selected to be adaptive to the input and output values, the best value of α in our system was 0.01, at the beginning of training process the system suggest initial values to θ_0 and θ_1 to form an initial hypothesis, then the system enters in iterations epochs to minimize the error or cost function value calculated in every iteration, the system will stopped when it reaches a specified value of error or a determinate number of iterations. The Figure 3 below illustrates the performance of optimization method, the best performance is MSE=0.0036 at the 25th iteration.

This stage of research was concluded with a linear function that used to produce an adaptive threshold to isolate the active zone in any studied *f*MRI image. We test the developed model on our testing dataset and realized an accuracy is about 96.28 %, the accuracy is calculated as a ratio between the numbers of selected activated zones (SAZ) and real activated zones (RAZ) see the following Equation 5.

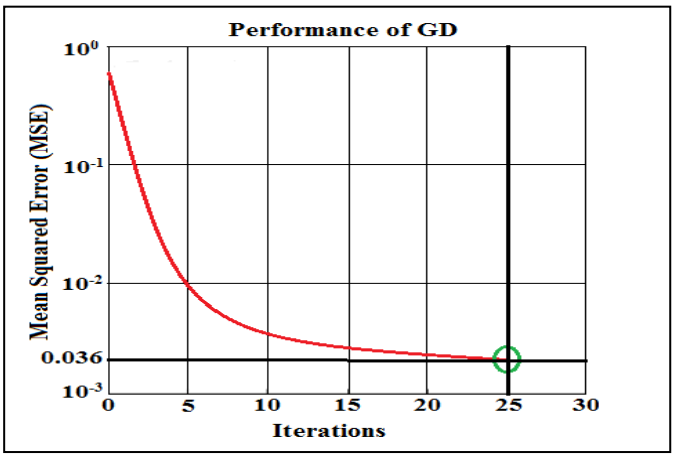

Fig. 3: Performance of optimization method (minimized the MSE by GD algorithm)

$$A_{CC} = \frac{SAZ}{RAZ} \quad (5)$$

Figure 4 below in its part (2) illustrates the result of applying the produced adaptive threshold on the studied image in part (1)

ISSN No:-2456-2165

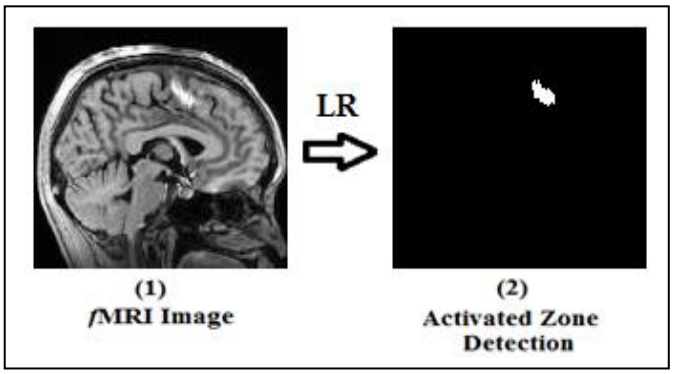

Fig. 4: Result of applying a produced adaptive threshold (2) on a studied image (1), by using LR algorithm

➢ Fuzzy C-mean Clustering

Fuzzy C-means Clustering algorithm (FCM) [14] is an our second approach to reveal the correct adaptive threshold to isolate the active zones in *f*MRI image, the first step is to represent the studied *f*MRI image using statistical Z-score basing on two statistical values of image, which are the mean value (MEAN) and the standard deviation (STD) using the Equation 6.

$$Z_{(i,j)} = \frac{Image_{(i,j)} - MEAN(image)}{STD(image)} \quad (6)$$

Where: i, j varies from 1 to the number of rows and columns in image map, respectively.

The statistical Z-score gave us the possibility to estimate the number of clusters K that the intensity values of image belong to it, we considered K as an input to FCM algorithm, which operates a set of iterations to classify all the pixels in image according to clusters centers (centroids), the algorithm begins by determining initial centroids and it calculates the distances between all centroids and image pixels, every pixel will belong to a cluster that realizes the minimum distance between its centroid and the pixel, the error in every iterationaction represents the sum of squared distances between cluster centroids and the pixels of image, the algorithm updates its centroids by measuring the mean of every produced cluster, and iterates to minimize the error, the process will be terminated in case of reached the desired error or the a selected number of iterations. Let we have n pixels in the image and we want to classify the pixels in k clusters, so the distance (D_k) between n pixels (P) and centroid (C_k) is calculated as illustrated in Equation 7 below:

$$D_k = \sum_i (P_i - C_k)^2 \quad (7)$$

Where: i varies from 1 to n

Error is calculated as illustrated in Equation 8

$$E_{rr} = \sum_{j=1}^{k} D_k \quad (8)$$

We obtained an important result from applying this approach is to determine the cluster of activation zones in *f*MRI image and their addresses in the image map. The outcome accuracy of this approach was calculated according to the Equation 5 that previously mentioned, and is reached 96.7. Figure 5below illustrates the performance of fcm on a studied *f*MRI image.

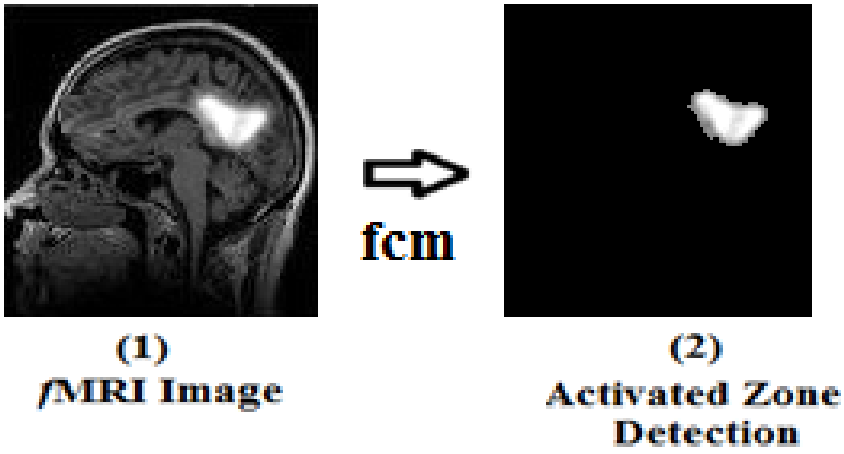

Fig. 5: Performance of fcm on*f*MRI image

B. Feature Extraction

After isolating the active regions in*f*MRI images, we have extracted four characteristic features over all images in our training dataset:

- The projection pattern (PP) of the studied *f*MRI image, which is a Vector represents the image in two projections, the Vertical and horizontal, the values in this feature takes one of two values, 1 for vertical and 0 for horizontal projection.
- Activation Score (AS) which it was represented in a vector of values that take one of two values 1 in case of activation and 0 in case of non-activation.
- The addresses of pixels in *f*MRI image on X-axis of Image map (Xind).
- The addresses of pixels in *f*MRI image on Y-axis of Image map (Yind).

These features were arranged in a 2D matrix of size (4 x 5040000) according to the amounts of pixels and features in our training dataset that have 65 *f*MRI images. Features matrix will be the input of our developed automatic classification system in the training stage. All the features vectors was normalized in everystudied image to take values in the range [0 1], both in training and testing stages.

C. Target Preparation

Our target represent the output of our developed automatic classification system in the training stage, it is 2D matrix (5 x 5040000) of elements, according to the number of five activities adopted in our dataset which are finger foot and lip movement (FFLM), overt verb generation (OVG), covert verb generation (CVG), overt word repetition (OWR) and landmark tasks (LT), and according to the number of pixels in all images of training dataset. Every vector in the target represent an activity task from the five studied activities, every element in every vector takes one of two values: 1 or 0 in cases of activation and non-activation respectively.

D. Automatic Classification System

➢ *Architecture*

The automatic classification system was build based on a neural network contains of three layers: the input layer has four nodes corresponding to the number of studied features, hidden layer has six nodes and output layer has five nodes corresponding to the classified behaviors. Figure 6 below illustrates the system architecture.

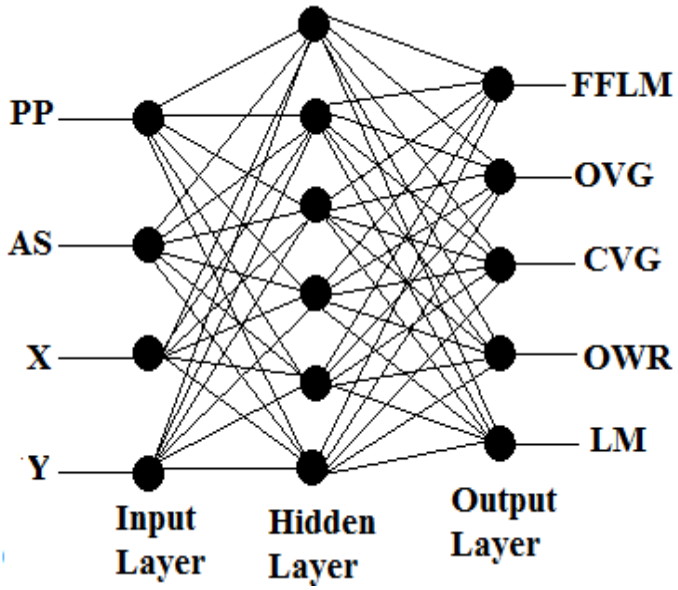

Fig. 6: Developed neural network architecture

➢ *Learning Method*

We tried many frameworks to learn our neural network system, Bayesian, Backpropagation (Bp) [3], Quasi Newton and Levenberg Marquardt, our experiments and evaluations proved that the performance of BP reached the best performance on our testing dataset.

It is also worth noting that when data passes through the three layers, it is processed to result in what is called the error function, which is the result of the difference between the expected (desired) outputs and the actual (real) outputs, and this output is called the error ratio and reaching it is the desired goal of using the algorithm. The Bp algorithm can summarized as illustrated in Diagram 1.

ISSN No:-2456-2165

1. Initialize weights (typically random)
2. Keep doing epochs
   a. For each example **e** in training set do:
      i. Forward pass to compute
         - O = neural- network –output
         - T: is the real output
         - .miss = (T-O) at each output unit
      ii. Backward pass to calculate deltas to weights
      iii. Update all weights
   b. End.
3. Until tuning set error stops improving.

Diag.1: Bp algorithm steps

It begins to compute deltas to weights from hidden layer to output layer, we used the derivation of activation function which is the logarithm sigmoid, the real output (T), the neural network output (O), the output of input layer (A), the input of input layer (I) and the learning rate (α) which chosen in our system equals to 0.01, let indicate the symbols (i), (j), (k) to the nodes of output, hidden and input layers, in our system i, j and k varies from 1 to 5, 1 to 6 and 1 to 4 respectively.

Firstly the algorithm calculates the deltas from hidden layer to output layer, see Equations 9, 10 and 11 below.

$$\text{delta}_{w_{ji}} = \alpha\ A_i(T_i - O_i)\ \text{Der}(O_i) \quad (9)$$

$$\text{Due to } O_i = \frac{1}{1 + e^{-A_i}}$$

$$\text{Der}(O_i) = O_i(1 - O_i) \quad (10)$$

$$\text{delta}_{W_{ji}} = \alpha\, A_i\,(T_i - O_i)O_i(1 - O_i) \quad (11)$$

Then the algorithm calculates deltas from input layer to hidden layer, see the Equations 12 and 13.

$$\text{miss}_j = \sum_i [A_i(1 - A_i)(T_i - W_{ji}) \quad (12)$$

$$\text{delta}_{ki} = \alpha\ I_k A_j(1 - A_j)\ \text{miss}_j \quad (13)$$

The learning algorithm achieved the best solution through 550 iteration with error about 0.0048, Figure 7 below illustrates the performance of backpropagation algorithm during the learning stage.

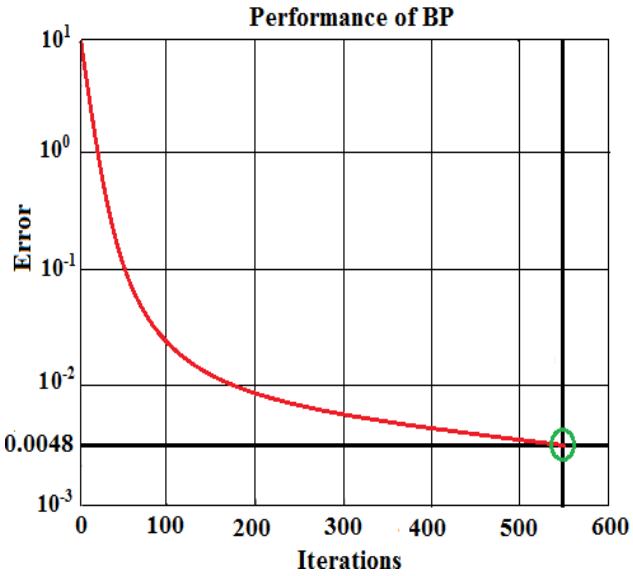

Fig. 7: Performance backpropagation learning algorithm

➢ *Testing and Results*

The developed system was tested by using testing dataset which represents 40% of our database, the testing dataset was not involved in learning stage, for every image, we extract four vectors of features according to the input layer of neural network.

The performance of system in testing stage was excellent, it realized a sophisticated capability to recognize 43 cases of behaviors from total 45 cases and it gave only 3 false alarms (false positive cases), in other hand it gave only 2 false negative cases.

We fixed an adaptive threshold to classify the values in the output vector, we consider the values >=0.5 represent positive cases and < 0.5 represent negative cases.TABLE I illustrates the results of testing stage. We used the symbols C_p, C_n, T_p, T_n, F_p and and F_n to represent the truly real positive, truly real negative, truly positive detected, truly negative detected, false positive detected and false negative detected cases respectively.

Cp	Cn	Tp	Tn	FP	Fn
45	45	43	42	3	2

Table 1: THE RESULTS OF TESTING STAGE

According to the results reported in TABLE I, we used a statistical functions to calculate the sensitivity (S_e), specificity (S_p) and accuracy (A_{cc}) these functions represent the system capacity to recognize correctly the positive cases, negative cases and both of them respectively, where the error(E_{rr}) represents the probability of both false positive and negative cases, see Equations 14, 15, 16 and 17 illustrate how we calculate S_e,S_p,$A_{cc}$and E_{rr}.The TABLEII reported the results of statistical evaluation process.

$$S_e = \frac{T_p}{C_p} \quad (14)$$

$$S_p = \frac{T_n}{C_n} \quad (15)$$

$$A_{cc} = \frac{T_P + T_n}{C_p + C_n} (16)$$

$$E_{rr} = 1 - A_{cc} \quad (17)$$

Se	Sp	Acc	Err
0.956	0.933	0.944	0.056

Table 2: The RESULTS OF STATISTICAL EVALUATION PROCESS

One of the efficient statistical methods to evaluate our results is using the receiver operating characteristics curve (ROC) which represents the relationship between the probabilities of true detected positive cases (S_e) and the probabilities of false positive detected cases (1- S_p), the probabilities used in ROC curve is calculated according to five thresholds, in the range [0 1]. we calculated according to every selected threshold the sensitivity and specificity of classifier, the obtained results proved that the best threshold is 0.5, <0.5 for the negative cases and >=0.5for the positive cases, see TABLE III, then we plotted ROC curve as illustrated in Figure 8, we also calculated the area under ROC (AUC) as an important index to evaluate the ROC curve efficiency, the AUC represents statistically the mean of obtained sensitivities at the selected thresholds, AUC in our system is 0.969.

Threshold	Se	Sp	1-Sp
0.1	1	0.60	0.40
0.2	0.978	0.64	0.36
0.3	0.978	0.71	0.29
0.5	0.956	0.933	0.067
0.6	0.933	0.978	0.022

Table 3: SENSITIVITIES AND SPECIFICITIES OF ROC

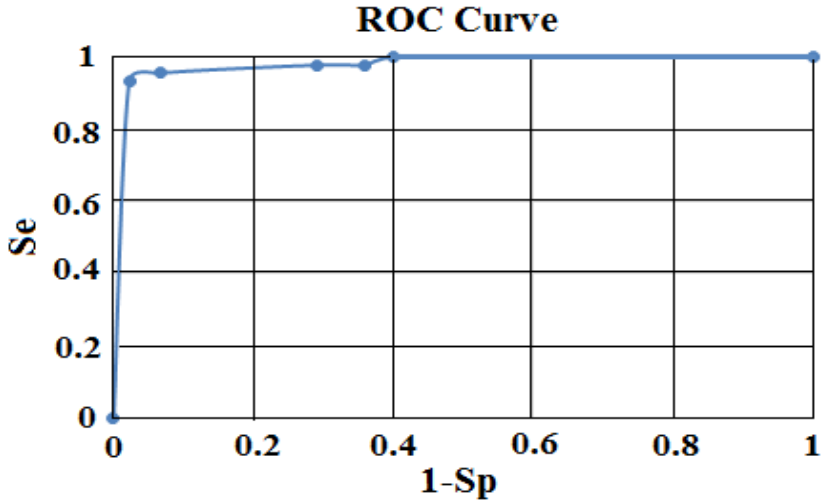

Fig. 8: ROC Curve

Figure 9 below illustrates all the steps of our developed system on a studied *f*MRI image, the image has an activated zone represents FFLM behavior, it is noted that the system classified clearly this behavior according to the activated zone in the image.

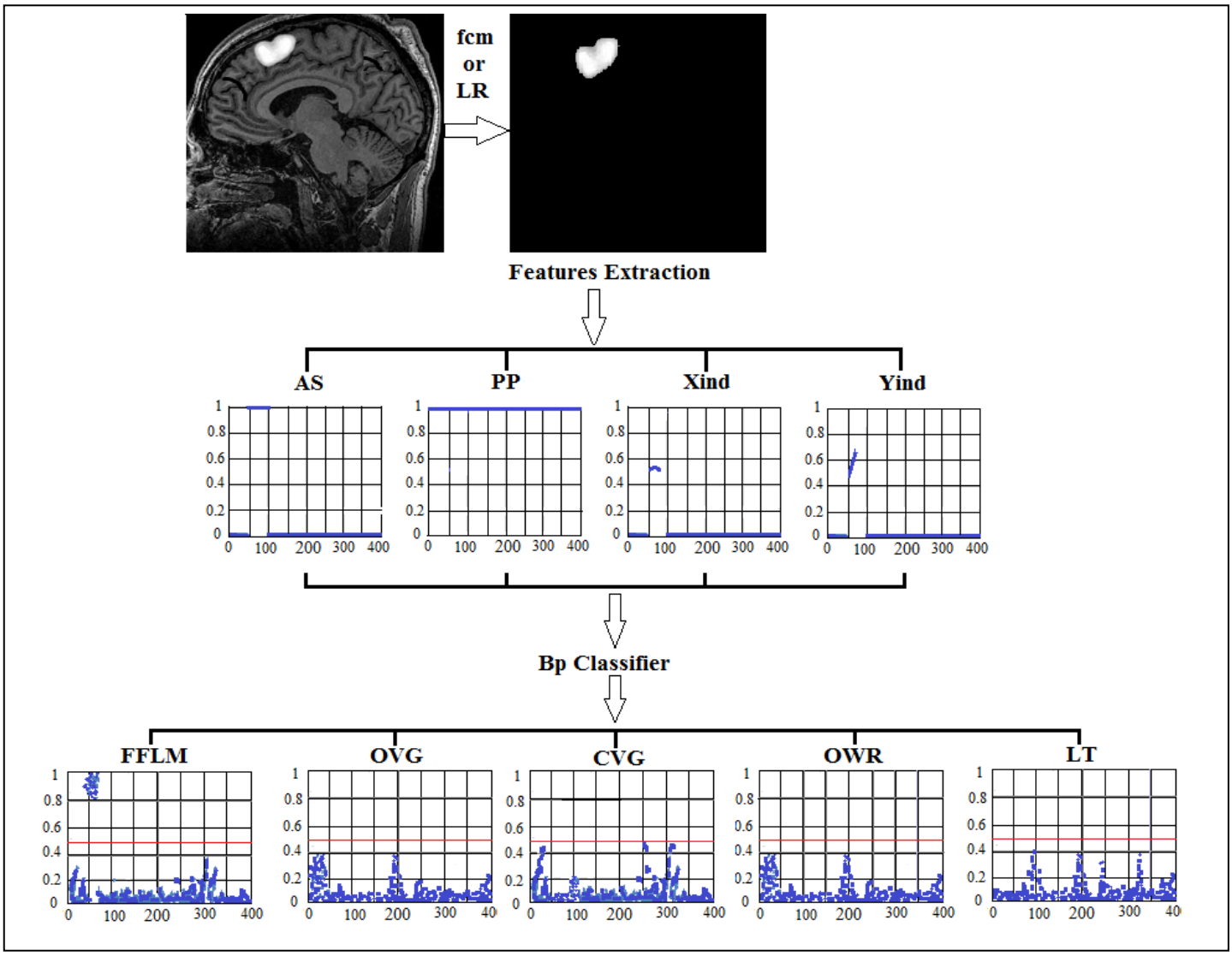

Fig. 9: Application of developed system on a studied *f*MRI image with an activated zone, the red line represents the threshold value of classification, FFLM behavior was recognized clearly

VI. DICUSSION

Through our methodology of research, we were able to introduce new techniques related to the field of processing and automatic analysis of digital images in order to extract the accurate information required to be known from the studied images, which were represented by *f*MRI images, this process facilitated to identify successfully and accurately the behaviors represented in the studied images, which is the desired goal of this research.

The results were obtained demonstrated a significant improvement in performance, compared to the results documented in the scientific research literature relevant to our research topic. We hope to enrich our research balance with more data in addition to the data that was used in the research, so our developed techniques become more generalized.

VII. DATA AVAILABILITY

Our major and first part of our dataset was obtained from the famous database (A test-retest *f*MRI dataset for motor, language and spatial attention functions), which contains 100 *f*MRI images with accordance to five different behaviors, this database is available free in [13], in the second part, we added other free 12 *f*MRI images obtained from Google, that were documented and classified manually in our dataset, for determining the behaviors presented in the added images and correlated to behaviors presented in our first part of dataset.

VIII. FUNDING STATEMENT

There is no funding for the research done, it is an individual effort by the author.

REFERENCES

[1.] Gaur, A. Augustyn, A. Zeidan, et,al. "Broca area", Encyclopaedia Britannica, Inc, Dec 15, 2022.
[2.] https://www.britannica.com/science/Broca-area
[3.] Gaur, A. Augustyn, A. Zeidan,et,al. "Wernicke area", Encyclopaedia Britannica, Inc, March 10, 2020. https://www.britannica.com/science/Wernicke-area
[4.] Singh, S. Kushwaha, M. Alarfaj and M. Singh, "Comprehensive overview of backpropagation algorithm for digital image denoising", Electronics, MDPI, vol.10, no. (11)1590, 15 pages, May 17, 2022.
[5.] A. Kirchhoff and L. Randy Buckner, "Functional anatomic correlates of individual differences in memory", Neuron,Cambridge, USA, vol.51, no.2, pp.263-274, July 20, 2006.
[6.] Candemir and K. Oğuz, "Change point detection ,methods for locating activations in functional neuronal images", BSEU Journal of Science, vol. 9, no.1, pp 541-554, May 30. 2022.
[7.] D.H. Maulud and A. M. Abdulazeez, "A review on linear regression comprehensive in machine learning", Journal of Applied Science and Technology Trends, Kurdistan, vol. 01, no. 04, pp. 140 –147, 2020
[8.] K. Jones, SC. Williams, D. Gasston, et al., "Isotropic resolution diffusion tensor imaging with whole brain acquisition in a clinically acceptable time", Hum Brain Mapping, Wiley Online Library,vol.15, pp.216-230, 2002.
[9.] G .Ganis, S. M. Kosslyn, S. Stose, W. L. Thompson and D. A. Y. Todd, "Neural correlates of different types of deception: An *f*MRI investigation". Cerebral Cortex, Oxford Academic, vol. 13, pp. 830-836, August 2003.
[10.] H. Hasan, E. ğlu , O. Puonti , C. Göksu Thielscher, et al., "On the reconstruction of magnetic resonance current density images of the human brain: Pitfalls and perspectives", Neuroimage, Science Direct, Elsevier,vol. 243, Article ID 118517, 15 pages, 2021.
[11.] H. Whitaker, "Concise Encyclopedia of Brain and Language", 1st Edition, e-Book ISBN: 9780080964997, Paperback ISBN: 9780081014516, January 14, 2010.
[12.] K. J. Duncan, C. Pattamadilok, I .Knierim and JT .Devlin, "Consistency and variability in functional localizers",Neuroimage, Science Direct, Elsevier, vol 46, pp. 1018-1026, July 15, 2009.
[13.] K. J. Gorgolewski, A. J. Storkey, M. E. Bastin and C. R. Pernet, "Adaptive thresholding for reliable topological inference in single subject *f*MRI analysis", Frontiers in Human Neuroscience,Switzerland, vol. 6, Article ID 245, pp. 1-14, August 25, 2012.
[14.] K. J. Gorgolewski, A. Storkey1 , M. E Bastin , I. R. Whittle, et al., "A test-retest *f*MRI dataset for motor, language and spatial attention functions", Gigascience,Oxford Academic,London, UK,vol.2, no.6, 4 pages, April 29 2013.
[15.] http://openfmri.s3.amazonaws.com/tarballs/ds000114_R2.0.1_raw.zip
[16.] L.Szilágyi, L.Lefkovits and D.Iclanzan, "A review on suppressed fuzzy c-means clustering models", Acta Universitatis Sapientiae, Informatica, Hungarian University of Transylvania,Hungary, vol.12, no.2, pp.302-324, Sep 27, 2021.
[17.] M. H. Lee, Nambeom Kim, Jaeeun Yoo, et.al, "Multitask *f*MRI and machine learning approach improve prediction of differential brain activity pattern in patients with insomnia disorder", Scientific Reports, Nature Portfolio,Springer Nature, vol.11, no.9402, 13 pages, Apr 30, 2021.
[18.] S. Ogawa, T. M. Lee, A. R. Kay and D. W. Tank, "Brain magnetic resonance imaging with contrast dependent on blood oxygenation",Proceedings of the National Academy of Sciences,USA, vol. 87, no 24, pp. 9868-9872, December 199